

SE 9500184

The Near-Field Transport in a Repository For High-Level Nuclear Waste

Leonardo Romero Aranguiz



Department of Chemical Engineering and Technology
Royal Institute of Technology
Stockholm, Sweden, 1995

TRITA-KET R21
ISSN 1104-3466
ISRN KTH/KET/R--21--SE

VOL.

The Near-Field Transport in a Repository For High-Level Nuclear Waste

Leonardo Romero Aranguiz



**Department of Chemical Engineering and Technology
Royal Institute of Technology
Stockholm, Sweden, 1995**

AKADEMISK AVHANDLING

som med tillstånd av Kungliga Tekniska Högskolan i Stockholm framlägges till offentlig granskning för avläggande av teknologie doktorsexamen tisdagen den 30 maj 1995, kl. 10.00 i K2, Teknikringen 28, KTH, Stockholm. Avhandlingen försvaras på engelska.

**ISSN 1104-3466
ISRN KTH/KET/R--21--SE**

Romero, L.: "The Near-Field Transport in a Repository for High-Level Nuclear Waste"
Department of Chemical Engineering and Technology
Royal Institute of Technology, S-100 44 Stockholm, Sweden.

ABSTRACT

The near field of a repository for high-level nuclear waste has been studied. The thesis is focused on the modelling of a redox front which is created when oxidants produced by a radiolytic process in a damaged canister escape to the surroundings, and on the design of a fast and flexible model to calculate the radionuclide transport in the repository. In addition, the thesis includes an attempt to validate the processes involved in the redox front model and a sensitivity analysis of the uncertainties in the parameter-values regarding the release of radionuclide from the Swedish KBS-3 repository.

The redox front model considers that the transport of oxidants in the clay surrounding the canister is by diffusion and that the transport in the fractures in the rock surrounding the repository is by flow with diffusion into the rock matrix. The advance of the redox front was calculated for three rates of production of oxidants. The range of the calculated travelled distances of the front is from a few centimetres to over a thousand metres. The long distances were, however, found to be unrealistic. The assumed radiolysis rates denoted low and high in the thesis are probably not realistic but can be seen as upper limits. Lower radiolysis rates are expected in the repository. Thus, it is unlikely that the redox front will ever move past the bentonite clay surrounding the canister and if it does the front may move less than 100 m. Several of the modelled processes were compared with data from an uranium mine in Poços de Caldas, Brazil.

The designed fast and flexible model to calculate the transport of radionuclides in the repository near-field uses a coarse compartmentalization of the repository by embedding analytical solutions in zones where other techniques, such as finite difference methods, would need a very fine discretization. The model allows us to consider simultaneously a multitude of pathways by which the nuclides are released from the repository. The concentration within the canister may be determined by the nuclide own's solubility or by a congruent dissolution of the fuel matrix. Only a few compartments are required to obtain a good accuracy in the calculated release. At some times for short-lived nuclides, the calculated releases are exaggerated. The error can be considerably reduced by increasing the number of compartments. Uncertainties in the release arising from the model are small in comparison to those arising from the variability in the parameter-values and material properties. Parameters such as hole size in the canister wall, uranium solubility, sorption, and the hydraulic properties of the fractured rock nearest to the canister are uncertain and variable. This will overshadow uncertainties due to model errors even for the coarse discretization.

Keywords: Repository, Model, Redox Fronts, Release, and Compartment.

ACKNOWLEDGMENTS

This work has been done at the Department of Chemical Engineering and Technology, Chemical Engineering, Royal Institute of Technology, Stockholm.

I am most grateful to my advisers, Professor Ivars Neretnieks and Dr. Luis Moreno, for their guidance and invaluable advice. The assistance and encouragement of all the staff at the Department of Chemical Engineering and Transport Phenomena is highly appreciated.

The work has been funded by the Swedish Nuclear Fuel and Management company (SKB). Thanks are expressed to SKB, and especially to Fred Karlsson, Tönis Papp and Patrick Sellin.

The thesis is based on the following papers:

- I** L. Romero, L. Moreno, and I. Neretnieks, Nuclear Technology, "Movement of a Redox Front around a Repository for High-Level Nuclear Waste," Nuclear Technology, In Press, 1995.
- II** L. Romero, I. Neretnieks, and L. Moreno, "Movement of a Redox Front at the Osamu Utsumi Uranium Mine, Poços de Caldas, Brazil," J. Geochem. Explor., 45: 471-502, 1992.
- III** L. Romero, L. Moreno, and I. Neretnieks, "Fast Multiple Path Model to Calculate Radionuclide Release from the Near Field of a Repository," Nuclear Technology, In Press, 1995.
- IV** L. Romero, L. Moreno, and I. Neretnieks, "The Fast Multiple Path Model NUCTRAN- Calculating the Radionuclide Release from a Repository," Nuclear Technology, In Press, 1995.
- V** L. Romero, L. Moreno, and I. Neretnieks, "Sensitivity of the Radionuclide Release from a Repository to the Variability of Materials and Other Properties," accepted for publication in Nuclear Technology, March, 1995.

CONTENTS

	Page
1 INTRODUCTION AND BACKGROUND	1
2 PROCESSES IN THE NEAR FIELD OF A NUCLEAR WASTE REPOSITORY	4
2.1 Redox potential in the repository and longevity of the canister	4
2.2 Near-field transport processes	5
2.3 Radiolytic process producing oxidants	6
3 REDOX FRONT MODELS	8
3.1 Modelling of a redox front in the KBS-3 repository	8
3.2 Model validation by observations in a natural analogue	13
3.3 Discussion of the redox front model	17
4 A MODEL TO CALCULATE RADIONUCLIDE RELEASE	18
4.1 Model formulation	18
4.2 Approaches used by the model	20
4.3 Managing the material balance in the compartments	22
4.4 Verification of the model	25
4.5 Illustrative calculations	26
4.6 Discussion of the model	28
5 IMPACT OF THE UNCERTAINTIES IN THE PARAMETERS ON THE RELEASE	29
5.1 Entities influencing radionuclide transport in the near field	29
5.2 Parameter sensitivity analysis	30
5.3 Discussion of the uncertainties in the release	33
6 CONCLUSIONS	34
NOTATION	35
REFERENCES	36
APPENDIX	39

1 INTRODUCTION AND BACKGROUND

Disposal of high-level nuclear waste in repositories located in deep geological formations is being studied by several countries in different parts of the world. These engineered repositories utilize the "multi-barrier" concept, whereby the waste is placed inside a series of engineered structures and natural barriers which act in concert to control the rate of release of radionuclides over long periods [1]. The repositories differ in the engineering design and in the geological formation where they are located and in the form of the waste that they contain. The waste is either spent fuel or vitrified waste packaged in a metal canister. The primary components of repositories are the near-field and the far-field subsystems. The near-field comprises the waste package, the backfill barrier system and the immediate surrounding rock, while the far-field comprises the natural barriers (e.g., host rock between the repository and the biosphere). These two sub-systems define a series of barriers that act to assure the safe isolation of nuclear waste. During repository evolution, there is a continuous decrease in the overall activity of the waste with time. A degradation of the package containing the nuclear waste is eventually expected and some radionuclides are therefore expected to return to the biosphere at some time in the future.

An important area addressed in the thesis is the radionuclide release in the near field of a repository of the KBS-3 type, the Swedish concept of a repository for spent nuclear fuel [2]. In this concept, the repository is located in crystalline rock. The copper canisters containing the spent fuel are placed in boreholes in the floors of tunnels at a depth of ~500 m as shown in Figure 1. At such depths, the rock is fractured with water-bearing fractures at typical distances of several metres. The nearest few metres around the tunnels are more fractured due to blasting damage and rock stress changes. The deposition holes are backfilled with compacted bentonite and the tunnels with a mixture of sand and bentonite. The canisters will eventually degrade and nuclides will leak out. The safety of the repository is ensured to a major extent by the longevity of the copper canister and the general performance of the near-field barriers.

The longevity of the copper canister is ensured by the reducing redox potential prevailing around the canister and the low ratio of moving water to solid rock. Copper is a near-noble metal under the groundwater redox conditions expected in deep granite, reducing and depleted of oxygen [3]. The canister may, however, initially be defective or damaged later by mechanical or corrosion processes.

The performance of the near-field barriers is assessed by the radionuclide release escaping from the repository. This release is controlled by the various processes occurring in the repository such as dissolution of the waste matrix, diffusion, advection, and chemical and sorption processes. In a repository where the backfill and the rock matrix have very low hydraulic conductivities, the radionuclide transport will occur mainly by diffusion. Transport by advection is restricted to the flowing water in the fractures in the rock. The waste matrix, mostly containing uranium dioxide, will dissolve when water comes into contact with the spent fuel and nuclides embedded in the matrix will be liberated. This process is controlled by the rate at which the uranium is released from the canister. The clay has a high porosity, even when compacted, and a good cation-exchange capacity. Therefore many sorbing radionuclides with short half-lives and high sorption properties may be delayed in the clay until they have decayed

to insignificant concentrations. Another process that will influence the radionuclide release is radiolysis of the water entering the canister. This process increases the solubility and lowers the sorption of some radionuclides by changing the redox potential in the repository from reducing to oxidizing. The change in redox potential is demarcated by the formation of a redox front in the repository separating the reducing from the oxidized zone. As more oxidants are produced in the canister, the front will advance, reaching the fractures in the rock. Thus redox-sensitive nuclides migrating with a higher solubility and lower sorption may be transported to a large extent in the far field if the oxidants reach the fractures in the rock.

The fundamental requirement of a suitable repository is that it should be relatively stable and its behaviour adequately predictable. The need for predictability arises from the need to be able to evaluate the long-term radiological safety of a disposal facility. Such an evaluation is necessary in order to demonstrate that a repository will comply with safety regulations. The essence of predictive safety assessments is to use models which describe, in a simplified but adequate fashion, the many processes leading to the degradation of the barrier system and the transport of radionuclides in the repository [1]. The ability to predict how these processes occur is the central issue in demonstrating the long-term safety of any waste repository.

The near-field transport calculations of a repository may be complex, considering that the nuclides migrate through several barriers and through various pathways, which may be different for different canisters depending on where the damage in the canister and the fractures in the rock are located. The complexity of this situation makes it difficult to obtain analytical solutions representing the whole picture of the near-field transport in the repository. Standard-numerical techniques such as finite difference methods require a detailed discretization of the system to be modelled. Therefore nuclide-release calculations would be very time-consuming if they were made using standard numerical techniques. In addition, possible variations in the system such as changes in the geometry, addition of new pathways, change in the transport properties and water flow rates in the fractures would also be laborious and time-consuming to set up in a detailed 3-D model. Thus, to circumvent these problems, there is a necessity for devising a model that allows the release calculations to be performed rapidly without loss of accuracy or confidence in the results obtained.

In this thesis, the evolution of a redox front in the near-field repository and the development of a fast multiple path model to calculate the radionuclide release from the repository are addressed. The redox front moves much more slowly than most of the dissolved nuclides and it is possible that the front locates close to the canister because of the limited production of oxidants in the canister. At this stage, we do not attempt to couple both models. The thesis consists of three parts. The first part gives an insight into the nuclear waste repository and the processes influencing the radionuclide transport in it. In the second part, the transport of oxidants giving rise to the movement of a redox front in the repository is modelled. The transport of oxidants in the clay surrounding the canister, produced by radiolysis of the water entering the canister, occurs by diffusion. In the rock, the transport of oxidants is modelled by flow in fractures, with diffusion into the rock matrix. This part includes the validation of the model concerning the processes involved in it. In the third and final part, the near-field transport is modelled as occurring through a network of resistances and capacitances coupled together like an electrical circuit network. The model takes into account all possible

pathways by which the nuclides are transported. To speed-up the calculations, analytical solutions are embedded in certain zones. The potential of the model is shown by making a parameter-sensitivity analysis of the KBS-3 repository in order to quantify uncertainties regarding the release to the far field.

2 PROCESSES IN THE NEAR FIELD OF A NUCLEAR WASTE REPOSITORY

Several processes may occur in the near field of a nuclear waste repository. Some processes, such as the transport of corrosive agents to the canister, will influence how long a canister will remain intact. Other processes will govern the radionuclide migration, such as dissolution, sorption, diffusion, and advection. In addition, radiolysis may change the chemical environment in and around the canister from reducing to oxidizing.

2.1 REDOX POTENTIAL IN THE REPOSITORY AND LONGEVITY OF THE CANISTER

Copper canisters are thermodynamically stable in pure water. Surface waters infiltrating downwards are oxidizing. They are depleted of oxygen by various mechanisms. Reactions with dissolved organic matter consume some oxygen and reactions with reducing minerals consume yet another part. The ferrous iron in Swedish crystalline rock varies between 1 and 8 wt% [4]. Deep groundwater in the Swedish bedrock is at a near-neutral pH and is depleted of oxygen. At 100 m depths and below, the waters are reducing, i.e. $E_h < -100$ mV [3]. The ratio of moving water to solid rock is small and the rock has a large redox capacity. In the backfill material surrounding the canister, bentonite, the ferrous iron varies between 0.1 and 1 wt% after an oxidizing heat treatment for the removal of organics [4]. The iron content in bentonite MX-80 is in the range of 2.5 to 3 wt% and 25 to 50% of this iron is divalent. After the bentonite has been subjected to a heat treatment, the fraction of ferrous iron is reduced to 5 to 10% [4]. A reducing redox potential will then prevail around the canister.

The canister will remain intact over a long time if the reducing redox potential around the canister prevails. The canister may, however, be initially defective or be damaged later by mechanical or corrosion processes. Initial defects may be eliminated by rigorous quality control, but there is always a chance that a defect in a canister is missed. The probability of this happening is <0.1% [5]. No mechanical failure is expected from pressure build-up inside the canister or from rock movements for millions of years [5]. The possibility that corrodants could diffuse to the container surface and cause corrosion must be considered. These oxidants could arise from entrapped air in backfill materials in the deposition hole and tunnel when it is sealed. Sulphide in the bentonite can make copper precipitate as copper(I) sulphide, allowing water to oxidize the amount of copper needed to form this precipitate. The supply of oxidants and sulphides from these sources is limited. There could be a continuous supply of sulphide from the groundwater which contains a level of ~ 0.5 mg/dm³ [6]. The canister longevity will thus depend on where corrosion takes place and on how rapidly corrosive substances are transported to the canister. Owing to the low supply of these corrodants to the canister, only local corrosion attack is of decisive importance for the life of the canister. The corrosion of the copper canister is then limited to small areas or pits. Pitting corrosion was recognized in the Swedish studies as a potential failure mechanisms for copper containers [2]. Corrosion analysis has, however, shown that there is no rapid mechanism that may lead to canister corrosion [6]. For the purpose

of the analysis of the nuclide transport in the near field, it is assumed that the canister has an initial damage with a size of 5 mm² [5].

2.2 NEAR-FIELD TRANSPORT PROCESSES

Processes governing radionuclide release in the repository are: rate of dissolution of the waste matrix, sorption, diffusion and advection processes. Radionuclides escaping from a damaged canister will leak out into the clay. They will migrate further into water-bearing fractures in the rock. Figure 1 schematizes the KBS-3 concept of a repository. It shows the small damage in the canister wall and four possible pathways for the migration of the radionuclide. The deposition hole is backfilled with compacted bentonite and the tunnel with a mixture of sand and bentonite. The clay and the rock matrix have very low hydraulic conductivities. Radionuclide transport in the clay will occur mainly by diffusion. Transport by advection is restricted to fractures in the rock.

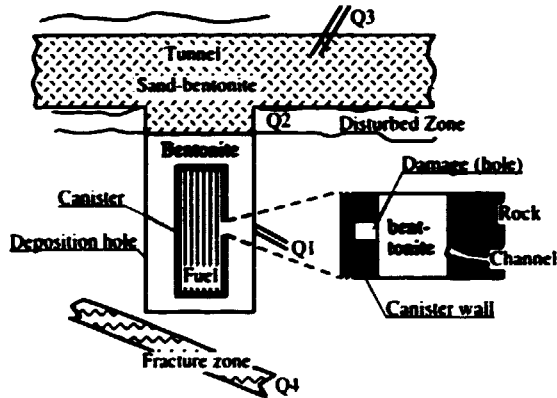


Figure 1 A schematic view of the KBS-3 repository design, showing a small hole in the canister and the location of the various escape routes.

Sorbing nuclides, during their transport through the backfill materials, may be retarded by sorption processes. The bentonite clay is made up of very small particles with a large surface area. The surface is chemically active and adsorbs water molecules strongly which makes the bentonite swell markedly [2 and 5]. Compacted bentonite has a very low hydraulic conductivity [7] and water flow under normal repository gradients is practically negligible. Ions dissolved in water will, however, move in the voids between the clay particles by molecular diffusion. Cations will adsorb on the clay particle surfaces because these are negatively charged. The negative surface charge will render it more difficult for the anions to enter the smallest passages due to electric repulsive forces.

The near-field rock is fractured and practically all the water flows in the fractures. The rock matrix is porous but the hydraulic conductivity is so low that practically no water flows through the rock matrix. The frequency of conducting fractures is small and varies between 1 per a few metres and 1 per nearly 100 m [8, 9 and 10]. Fractures are not open over their whole surface. Only small parts of a fracture conduct water in what is often called channels [11 and 12]. The channel transmissivity varies within a wide range. This means that not all deposition holes will be intersected by a fracture and only a few will be intersected by a channel with a high flow rate.

The safety assessment of a spent nuclear fuel repository requires information concerning the rates at which radionuclides will be released from the fuel elements after groundwater breaches the fuel cladding and contacts the fuel. Three main release mechanisms have been identified, operating on different time scales [13]. First, there is the rapid release of soluble fission products (e.g., cesium and iodine) from the fuel/cladding gap as soon as groundwater penetrates the fuel cladding. Second, there is a leaching of fission products (e.g. cesium, iodine and technetium) from the fuel grain boundaries. Third, there is the very slow release of radionuclides from the fuel matrix due to the slow dissolution of the UO_2 grains.

The dissolution of the fuel matrix controls the release of the major fraction of the radionuclide inventory. Radionuclides are released as the fuel matrix dissolves. If the transport rate of the uranium through the buffer is slow and the UO_2 is the thermodynamically stable uranium solid, the rate of dissolution of the fuel matrix is limited by the solubility of the UO_2 . If the UO_2 is not the thermodynamically stable uranium solid, the rate of dissolution of the matrix may be controlled by kinetic transformation rates rather than by the transport of dissolved uranium away from the canister [14].

The solubility of uranium in the spent fuel is strongly influenced by the redox conditions at the fuel surface, which may be changed by radiolysis. The radiolysis will locally develop an oxidizing environment in which the uranium has a solubility of the order of milligrams per litre instead of micrograms per litre or less under reducing conditions [15]. The uranium U(IV) is oxidized to U(VI) which can dissolve at the higher solubility limit. When the radiolysis rate and the resulting formation of U(VI) are larger than what can be released from the canister, new crystalline phases will be formed. The re-crystallized uranium will not necessarily re-incorporate the other radionuclides which are originally embedded in the UO_2 matrix. Under these conditions, the upper limit for the escape rate of the nuclides will be determined by their own solubility. In the clay, as a consequence of the radiolysis, radionuclides escaping from the canister will move more rapidly because they will be less retarded in the oxidized pathways.

2.3 RADIOLYTIC PROCESS PRODUCING OXIDANTS

Water penetrating a damaged canister may reach the gap between the fuel pellets and the Zircaloy cladding, wetting the spent nuclear fuel. The radiation, mainly the alpha-particle radiation, will split the water into hydrogen and oxidizing agents, mainly hydrogen peroxide:



The range of the alpha-particle radiation in water is ~0.03 mm [16], i.e., of the same magnitude as the water film in the gap between the fuel pellets and the Zircaloy tube. This short range means that the radiolysis is limited to the water in the gap around the fuel pellets and its magnitude is directly proportional to the exposed surface area ($\approx 144 \text{ m}^2$ per canister). This available surface area and the thickness of the water film in the gap determine how much water may be penetrated by alpha-particle radiation. There are many uncertainties involved when trying to estimate the net radiolytic productions of oxidants. This is reflected in the very wide range of estimates in Table I.

Table I Estimated Values of The Hydrogen Peroxide Production Per Canister in One Million Years. This Corresponds to a G-Value of ~1 for the Production of Hydrogen [16].		
Production	(mol)	Reference
low	144	Christensen and Bjergbakke [16]
high	29 000	Christensen and Bjergbakke [16]
small	144 / 100	Neretnieks and Faghihi [17]

Note: low and high are for the case when there is no limitation in the water supply to the canister. Small is for the case when the amount of water is limited. G-value means the amount of oxidant (reductant) per unit of energy.

The hydrogen production resulting from alpha- and beta-particle radiation, in water in a copper canister, has been estimated by Christensen and Bjergbakke [16]. They found that the beta-particle radiation produces a great number of radicals that aid the recombination of the radiolysis products and that the redox couple Fe(II)/Fe(III) catalyses this recombination. Calculations were made for an Fe(II) concentration in water of 0.6 mg/l, which is within the range of concentrations found in Swedish groundwater, 0.3 to 1 mg/l [5]. In this case, the oxidant production is 144 mol H₂O₂ per canister in one million years. In a hypothetical case, in which no iron is dissolved in the water, the production of oxidants per canister would increase to 29 000 mol of H₂O₂ during the same period of time. These two productions would be obtained if there were no limitations on the supply of water and if water filled all the available spaces in the canister. Neretnieks and Faghihi [17], on the other hand, proposed a production of oxidants by radiolysis of 1.44 mol in one million years, which is two orders of magnitude lower than that estimated by Christensen and Bjergbakke. This small oxidant production is obtained by limitations in the amount of water to be radiolysed. The pressure produced by the hydrogen gas in the interior of the canister which will limit the inward transport of water, as is the case when the canister is locally corroded. The formation of corrosion products in the gap around the fuel pellets reduces the amount of water in the gap available for radiolysis.

3 REDOX FRONT MODELS

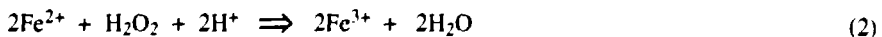
The environment of deep repositories for high-level nuclear waste is a reducing environment, but it may be changed by the escape of oxidants from the canister produced by the radiolysis of the water in contact with the spent fuel. These oxidants may oxidize the reducing species in the bentonite and later in the rock. A redox front will be formed demarcating the oxidized and reducing zones. Under oxidizing conditions, uranium dioxide and other redox-sensitive elements are oxidized to a higher oxidation state and become more soluble. The sorption in the backfill material becomes lower. These nuclides migrating with a higher solubility and lower sorption may be transported to a large extent in the far field if the oxidants reach the fractured rock. Nuclides having a much lower solubility in a reducing environment than in an oxidizing environment, such as U, Np, and Tc, will precipitate at or just downstream of the redox front.

3.1 MODELLING OF A REDOX FRONT IN THE KBS-3 REPOSITORY

The approach taken here has been to set up a mathematical model of the movement of the redox front in the clay, bentonite, surrounding the canister and in the fractured rock around the deposition hole. In the clay, the movement of the redox front is calculated by a mass balance involving the reductant capacity of the clay and the oxidant production in the canister. In the fractured rock, the transport of the oxidants is modelled as taking place through fractures.

The Model

The starting point for the modelling is the breach of the canister containing the radioactive waste. Once the canister has been breached, water intrudes into the canister and the spent fuel becomes wet. The radiation, mainly the alpha-particle radiation, breaks down the water molecules into oxidants, mainly hydrogen peroxide, and reductants, mainly hydrogen. The hydrogen is assumed to diffuse away from the canister due to its low reactivity, whereas the oxidants will react with the reducing species in the canister and, if the amount of oxidants is sufficiently large, with the reducing species outside the canister. The model assumes that all oxidants produced by the radiolysis of the water escape from the canister and react with the ferrous mineral in the clay. When the oxidants reach the rock, they may diffuse into the unoxidized clay, into the rock or be removed by the flowing water in the fractures intersecting the repository hole. In the fracture, the oxidants diffuse into the rock matrix and react with the reducing species in the rock. The redox reaction of the oxidants with the reducing species in the clay and in the rock matrix may be generalized by:



where the various oxidants, including the oxidized nuclides, are summarized and denoted by the hydrogen peroxide formula H_2O_2 . As this reaction is known to be instantaneous and irreversible, a very sharp redox front is formed separating the oxidized zone from the reducing zone.

General Assumptions

Several assumptions were made when modelling the transport of oxidants from the canister. The main are:

- a) The canister is locally damaged and oxidants escape from the canister through a small hole.
- b) The deposition hole in the repository is intersected by a fracture. The location of this fracture is opposite to the damage in the canister wall.
- c) Oxidants are produced only after the canister is breached.
- d) Oxidants do not react with the canister material.
- e) Only diffusive transport takes place in the clay surrounding the canister.

Redox Front in the Bentonite

The oxidants escape through the small damage in the canister wall into the bentonite where they react with the ferrous iron available there. In addition to the above assumptions, it is assumed that all reducing species (ferrous iron) in the bentonite are available to react with the oxidants [7]. Figure 2 shows the spread of the redox front from the small hole in the canister wall. The time needed to oxidize the reducing species in the bentonite is calculated by a mass balance between the reducing capacity of the bentonite and the rate of production of oxidants, for the time interval between the breach of the canister T_1 and the time at which the oxidants reach the rock T_2 :

$$q_0 f V = \int_{T_1}^{T_2} N^c dt \quad (3)$$

where V is the volume of the oxidized clay just before the oxidants reach the fracture mouth in the rock, q_0 is the concentration of the reducing species in the clay, and f is the stoichiometric factor for the redox reaction. The volume V of oxidized clay is determined by the relative location of the hole in the canister and of the fracture intersecting the repository hole. If the hole and the fracture are opposite each other, we can approximate the shape of the oxidized clay by a hemisphere (see Figure 2).

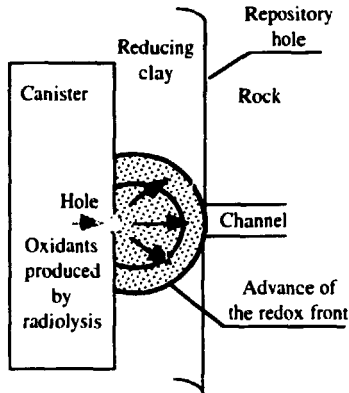


Figure 2 The advance of the redox front when the canister is locally damaged. The arrows show the direction of the spherical spread of the redox front.

At this stage, the calculation of the movement of the redox front is limited to the clay. The time needed for the redox front to reach the fracture mouth for two breaching times is shown in Figure 3.

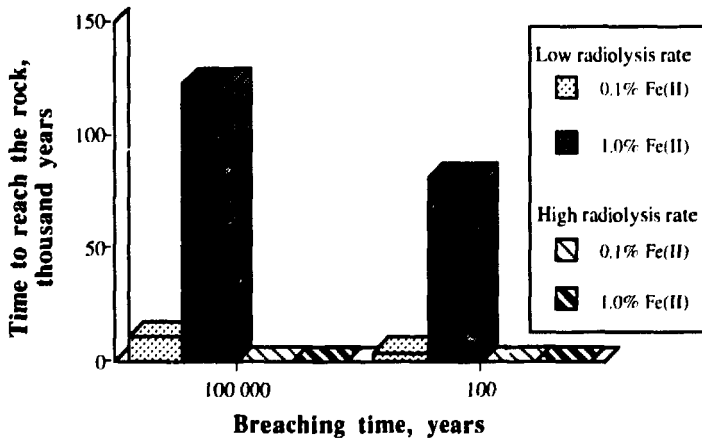


Figure 3 The canister is locally damaged. Times are given for the redox front to reach the rock, for high and low radiolysis rates. For the small radiolysis rate, the oxidants never reach the rock and are not shown.

For a content of Fe(II) of 0.1 wt%, the reducing capacity of the clay in the hemisphere is equivalent to a production of ~2.5 mol of H₂O₂, which is approximately twice the productior

oxidant produced at the small radiolysis rate (1.4 mol in one million years). Thus, for small radiolysis rates (<2.5 mol/10⁶ years), the reducing capacity of the clay given by the content of ferrous mineral (0.1 to 1 wt%) will suffice to entrap the redox front within the clay. For the other production rates (low, 144 mol/10⁶ years and high, 29 000 mol/10⁶ years), the time to reach the fractured rock is short, except for the low production rate and with an Fe(II) content of 1.0 wt%.

Redox Front in the Fractured Rock

The rock is modelled as a fractured medium with sparse channels in the fracture planes. In the fracture, the oxidants are transported by advection. From water in the fracture, they diffuse into the rock matrix and react with the ferrous iron as shown in Figure 4. The advective transport of a species along a fracture, neglecting the axial dispersion [18], is:

$$\frac{\partial c^f}{\partial t} + u \frac{\partial c^f}{\partial z} + \frac{f}{m} \frac{\partial q}{\partial t} = 0 \quad (4)$$

where c^f is the concentration of oxidants in the water in the fracture, u is the water velocity in the fracture, q is the concentration of oxidized Fe(II) in the rock, and m is the ratio of water volume in the fracture to the solid volume of the rock. The first term in this equation accounts for the accumulation of oxidants in the fracture, the second accounts for the transport by flow in the channel, and the third stands for diffusion into the rock matrix.

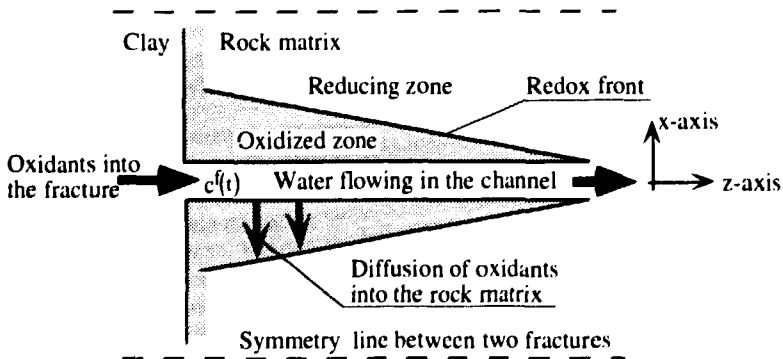


Figure 4 A schematic view of the channelling model. The z axis is in the flow direction and the x axis in the diffusion direction.

In the rock matrix, the diffusion transport is modelled as diffusion from two water flow channels into a slab of thickness S . The rate of movement of the redox front in the direction perpendicular to the wall of the fracture is:

$$\frac{dx}{dt} = - \frac{D_e}{q_o f} \left(\frac{dc_p(x,t)}{dx} \right)_{x_r} \quad (5)$$

where D_e is the effective diffusivity, x_r is the location of the redox front, and c_p is the oxidant concentration in the pore water. The concentration gradient is evaluated by assuming a quasi-steady state due to the high redox capacity of the rock compared to the intruding oxidants from the fracture. Combining Equations (4) and (5), analytical solutions are obtained for the time interval before and after the redox front has reached the centre of the slab at the clay-rock interface at the mouth of the fracture. Here, only the solution for the time interval before the front reaches the centre of the slab is shown:

$$\frac{x}{S/2} = \sqrt{\frac{2 D_e}{(S/2)^2 \cdot q_o \cdot f} \int_{T_2}^T c^f(t) dt} = - \frac{D_e}{(S/2)^2 m u} z, \quad t \leq t_{cr} \quad (6)$$

where x is the penetration of the redox front into the rock from the fracture, z the penetration distance along the fracture, and t_{cr} is the time to reach the centre of the slab at the clay-rock interface, which may be calculated from Equation (5). At the fracture mouth, it is assumed that all the oxidants in the fracture intersecting the deposition hole are transported into the one-metre-wide channel downstream. The time-dependent concentration of oxidants, $c^f(t)$, can then be calculated from the amount of oxidants that actually diffuse into the fracture and from the water flow rate in the channel.

The fraction of oxidants diffusing into the fracture is determined by considering the further oxidation of the clay and its uptake into the rock. Details of the calculations are shown in Paper I. Once the fraction of oxidants into the fracture is determined, the distance reached by the tip of the redox front along the fracture is calculated using Equation (6). The tip of the front reaches further (200 to 1500 m) when a high production rate is assumed. For a low production rate, short distances are reached (2 to 50 m), see Figure 5. These large differences in distances are determined by the amount of oxidant intruding into the fracture. The tip of the redox front advances a longer distance if the channel has a high flow rate. The maximum penetration of the redox front into the rock matrix is of the order of a few centimetres.

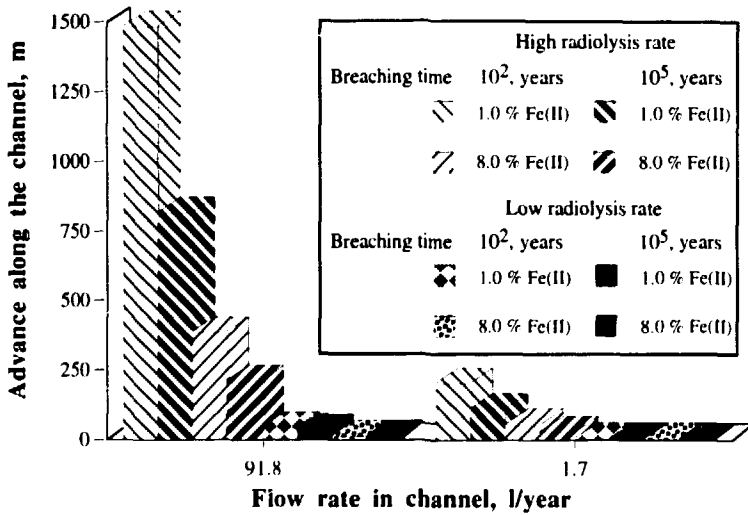


Figure 5 The advance of the tip of the redox front along a channel in the fracture after one million years for two channels with different flow rates. The canister is locally damaged.

3.2 MODEL VALIDATION BY OBSERVATIONS IN A NATURAL ANALOGUE

The calculations predict redox front movements over long times and distances. Such fronts have been found in nature. One such occurrence is in the Osamu Utsumi uranium mine at Poços de Caldas in the state of Minas Gerais, Brazil. Here, the fronts are clearly seen in the open pit uranium mine. In the mine setting, many processes were found to be similar to those processes which are thought to take place in a repository for high-level nuclear waste, such as the formation and movement of the redox front and the precipitation of uranium dioxide at the redox front.

The redox front at Poços de Caldas is created by infiltration of rainwater containing dissolved oxygen. The redox front appears as "fingers", declining at a certain angle downward from the ground surface. The shape of these fingers, formed mainly by the oxidation of pyrite in the rock, shows that the solute transport occurs mainly by advection in fractures, associated with diffusion of the oxygen into the surrounding rock. The mechanisms involved in the formation of redox fingers and wedges are illustrated in Figure 6. Oxygenated rainwater infiltrates into the ground, and some of it flows in the rock matrix with a local flow rate that is determined by the hydraulic conductivity of the rock. In the fractures and in fracture zones, the conductivity is higher and more water will flow. The water that flows in a fracture comes either from direct infiltration from the ground or from the inflow through the rock matrix. This is illustrated by the flow vectors that show the direction of the water flow. The redox front forms a wedge around the fracture, owing to the water flow. In addition, the water, which has

reached the fracture by flowing through either the fracture from the beginning or through already oxidized rock, still contains oxygen. As the water flows down into the reducing rock, the oxygen diffuses into the rock matrix and reacts with the pyrite.

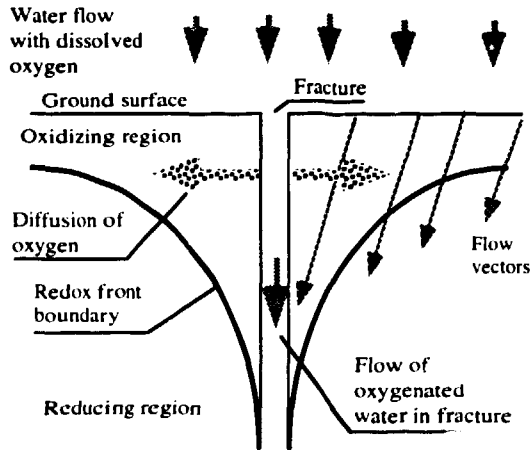


Figure 6 Oxygenated water flows in a fracture, and dissolved oxygen diffuses into the rock matrix, where it reacts with the pyrite at the redox front.

To explain the location of the redox front in Poços de Caldas, several models, with various levels of complexity, were used. These models, both for porous and fractured media, are summarized in Table II. To account for erosion, the velocity of the front is superimposed on the velocity of erosion. When the process is allowed to go on for a long time, in models whose velocity of advance is time-dependent, a stationary state develops and the depth of the front stabilizes at a constant distance from the ground surface.

Table II A Summary of the Final Equations of the Various Redox Front Models		
	Front Velocity v_f	Advance of the front x (into matrix) and z (along fracture)
Porous medium		
Diffusion	$\sqrt{\frac{2D_e c_o}{f q_o}} \frac{1}{\sqrt{t}}$	$x = \sqrt{\frac{2D_e c_o}{f q_o}} \sqrt{t}$
Advection (constant flux)	$\frac{u_o c_o}{q_o f}$	$x = \frac{u_o c_o}{q_o f} t$
Fractured medium		
constant flux	$\frac{u_o (S/2)}{D_e} \sqrt{\frac{D_e c_o}{2f q_o}} \frac{1}{\sqrt{t}}$	$z = \frac{u_o (S/2)}{D_e} \sqrt{\frac{2D_e c_o}{f q_o}} \sqrt{t}$
flux varies inversely with depth to an exponent n	<p style="text-align: center;">Front velocity</p> $\frac{1}{2(n+1)} \left\{ \frac{2c_o (S/2)^2}{D_e q_o f} [(n+1) z_o^n u_o] \right\}^{\frac{1}{2(n+1)}} \frac{1 - 2(n+1)}{2(n+1)} \{t\}^{\frac{1}{2(n+1)}}$ <p style="text-align: center;">Advance of the front</p> $z \approx \left\{ \frac{2c_o (S/2)^2}{D_e q_o f} [(n+1) z_o^n u_o] \right\}^{\frac{1}{2(n+1)}} \{t\}^{\frac{1}{2(n+1)}}$	

Note: c_o is the constant concentration at the inlet, q_o is the initial concentration of the reducing species, D_e is the effective diffusivity, f is the stoichiometric factor for the reaction, S is the fracture spacing, t is time, u_o is the infiltration flux at the ground surface, z_o is an arbitrary depth at which the infiltration flux is constant, n is the exponent utilized in the equation for the variation of the water flux with depth.

Redox Front at the Uranium Mine in Poços de Caldas

For the porous medium approach, it may be noted that the velocity of advance of the redox front, due to diffusion, decreases with time, whereas for transport by flow, the velocity is constant. The advance of the front by diffusion would be ~1 m in one million years. If erosion is taken into account, the front would stabilize only a few centimetres from the surface. When water flows through the rock (advection), it is conceivable that the front movement would just balance the erosion. If erosion is slightly faster, the front disappears, and if the erosion is slower for a long period of time, the front could reach very large distances.

The fingering in the rock and the depths reached by the redox front can be explained by oxygenated water flowing through fractures or zones with high hydraulic conductivity. The fractures are independent and have different flow rates. Several models were applied. In one, it was assumed that the flow rate in a given fracture is constant, independent of the depth. For

this approach, the depths reached by the redox front could be extremely large, even accounting for erosion. The reason for this is the assumption of a high and constant water flow rate in the fractures and the fact that they are assumed to be independent of each other. In another model, the stream tube concept was used, in which the water flow rate decreases with depth. Holmes et al. [19] found that the flux varies inversely with depth in a manner which might be approximately represented by an exponent "n" of ~ 0.5 . There are, of course, considerable variations in different locations. The infiltration flux u_0 at a depth of 1 m was assumed to vary between 0.1 and 1 $\text{m}^3/\text{m}^2\cdot\text{year}$. Figure 7 shows that the depth reached by the redox front accounting for erosion can vary considerably with the flux and the exponent n.

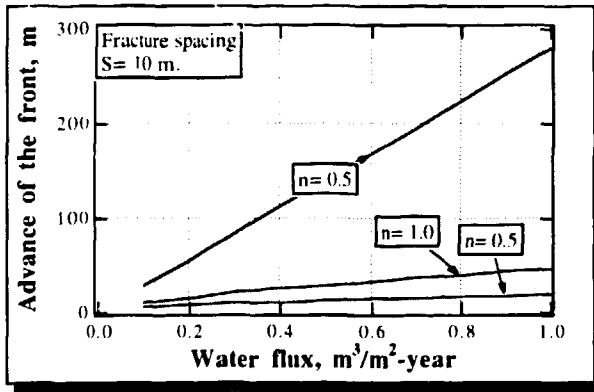


Figure 7 Steady state advance of the redox front in the fracture as a function of the infiltration flux at the ground surface for various values of the exponent in the equation of the flux varying inversely with depth. Erosion is assumed to be 30 m per million year.

Process Validation by Observations in Poços de Caldas

Simple calculations can explain the movement of the redox front in general terms, but there is a great simplification of the processes known to be occurring at such fronts [20]. This was evident in the study of the movement of the redox front at Poços de Caldas, where some of the simplest models were quite useful for analysing the ongoing processes. Simple mass balance models help to give an insight into some of the main processes. Concerning the movement of the redox front, the Poços de Caldas natural analogue study showed that matrix diffusion is clearly present as a mechanism to access the interior of the rock matrix. Channelling is also clearly present over considerable distances, and channels may carry some water and its dissolved constituents further than does the average flow rate. Dissolution and precipitation of uranium at the redox front is clearly in evidence. The fact that oxidizing species are reduced when they reach the redox front is validated by the field observations. Basic assumptions of model mechanisms such as water flow in fractures and diffusion into the rock matrix are also validated by the field observations.

3.3 DISCUSSION OF THE REDOX FRONT MODEL

The redox front model predicts long distances of advance of the oxidants escaping from the canister in the fractured rock. The travelled distances are conditioned by the amount of oxidants intruding into the fracture, and the wetted surface area in the channel, from which the oxidants diffuse into the rock matrix.

The amount of oxidants intruding into the fracture will depend on the rate of radiolysis by which the oxidants are produced in the canister. It will also depend on the Fe(II) content in the clay and rock. The radiolysis rates are not well known. A range of four orders of magnitude in the rate of radiolysis was used to bracket possible rates. Some recent field observations in a uranium ore body at Cigar lake [21] indicate that radiolysis is about two orders of magnitude less than what would be the "high" case. A factor of uncertainty also arises in assessing the movement of the front along the channels. The magnitude of the channel surfaces is poorly known. A channel width of 1 m has been used here. The channel width may well be less and the front would then move further. On the other hand, individual channels are probably not isolated for long distances but are parts of a complex network. In this case, the channel divides into other channels, and the oxidants get access to more flow-wetted surface, from which they can migrate into the rock matrix by diffusion.

In spite of these uncertainties, it is unlikely that the redox front will ever move past the bentonite. If it does, the tips of the redox front may move <100 m in a channel with a high flow rate. No credit has been given to the large amount of copper in the canister, which could act as a reducing agent. If it did react, no redox front would form in the bentonite even at the highest rate of radiolysis.

4 A MODEL TO CALCULATE RADIONUCLIDE RELEASE

In a repository of the KBS-3 type, the radionuclide transport occurs mainly by diffusion through a barrier system and through various pathways depending on the location of the water-bearing fractures in the rock. The escape of the radionuclide from the canister is through a small hole. A view of this repository is shown in Figure 1, where the possible pathways are: directly to the water in a fracture intersecting the deposition hole Q1, up to the disturbed zone around the tunnel Q2, into the tunnel backfill and further to a fracture (zone) intersecting the tunnel Q3, and through the rock to a nearby fracture or fracture zone Q4.

The physical geometry of the repository, the various materials through which the nuclides are transported, and the various possible pathways make it difficult to express the nuclide transport in an analytical form. Moreover, possible variations in the system make it tedious and time-consuming to set up and run detailed three-dimensional transport calculations using conventional numerical techniques. To circumvent these problems, a new technique was developed. This technique uses the advantages of the Integrated Finite Difference method [22] combined with analytical solutions at locations where standard numerical techniques would need a very detailed discretization. This technique has been used to develop a compartment model. The model accounts for the dissolution rate of the waste matrix and the transport of the radionuclides in the various materials. The transport is by diffusion. Advection is confined to the fractures in the rock. A verification of the model and some illustrative examples of calculations are presented.

4.1 MODEL FORMULATION

Radionuclides leaking from a damaged canister spread into the backfill material surrounding the canister and then migrate through different pathways into water-bearing fractures in the rock surrounding the repository. If the backfill and other materials surrounding the canister have a low permeability, water flow is excluded from these materials and the solute transport is only by diffusion. Some nuclides will be delayed by sorption on the materials through which they move and those nuclides with short half-lives may decay to insignificant concentrations before they reach the flowing water in the fractures in the rock.

The mathematical formulation conceptualizing the model arises from the material balance for a single nuclide over a unit volume. This formulation describing the physical processes that determine the nuclide transport results in two equations. The first equation models the transport of the solid dissolved, including the sorption in the solid material. The second equation models the amount of nuclide as solid inventory. These two equations coupled by a dissolution term q_d are expressed as follows:

$$K \frac{\partial c}{\partial t} = q_d + \nabla \cdot D_c \nabla c - K \lambda c \quad (7)$$

$$\frac{dm}{dt} = - m \lambda - q_d \quad (8)$$

where λ is the decay constant, c is the concentration in the pore water, m is the mass of nuclide as solid (as precipitate) in the unit volume, and K is a distribution coefficient. This coefficient K considers the nuclides dissolved in the water and sorbed in the solid, and can be expressed as:

$$K = \epsilon_p + (1 - \epsilon_p) k_d \rho \quad (9)$$

where ϵ_p is the porosity of the material, ρ is the density of the solid material, and k_d is the nuclide sorption coefficient.

For the purpose of numerical simulation, it is more convenient and less restrictive to formulate the model in terms of integrated finite differences [22]. Here, the concept of "compartments" is introduced to define the discretization of the system. The barrier system is then discretized into compartments. Average properties are associated over these compartments with representative nodal points within the compartment. Within a compartment the average properties such as concentration vary smoothly. The compartments may have any shape, but are of the same material. The material balance over a compartment connected to some other compartments for a fully dissolved single species is then expressed as follows:

$$V_i K_i \frac{dc_i}{dt} = \sum_{j \neq i} \left(\frac{A D_c}{d} \right)_{i,j} (c_j - c_i) - V_i K_i \lambda c_i \quad (10)$$

$$\text{where } \left(\frac{A D_c}{d} \right)_{i,j}^{-1} = \left(\frac{A D_c}{d/2} \right)_i^{-1} + \left(\frac{A D_c}{d/2} \right)_j^{-1} .$$

V_i is the volume of the compartment, A is the cross-sectional area used for diffusion, and d is the diffusion length. The left-hand side accounts for the accumulation of the species in the water and the solid by sorption. The right-hand side accounts for the diffusive transport from one compartment to the adjacent compartments and the degradation rate of the species by decay. The sub-index "i,j" defines the radionuclide flow from compartment "i" to the adjacent compartment "j". Equation (10) can be re-written and expressed in matrix form as:

$$\frac{d\bar{c}}{dt} = \bar{F} \cdot \bar{c} \quad (11)$$

where \bar{c} is the vector of concentrations of dimension equal to the number of compartments, and \bar{F} is the matrix of coefficients accounting for the transport and decay of the species. This system of equations is solved using standard numerical techniques based on the Gear implicit multi-value method [23]. The solution is straightforward once the initial conditions have been

defined. These conditions are defined by the amount of the species dissolved and the amount of the species existing as solid inventory in the compartments. The default initial condition is zero concentration for all compartments, except for the compartment acting as a source where the initial conditions are determined by the inventory and the solubility of the species.

To handle the inventory in the source, two situations are considered:

- a) nuclides are found free of the fuel matrix in the canister. They may then be handled as being independent of each other with the nuclide inventory and the nuclide's own solubility as only limitations; the solubility limit approach.
- b) nuclides are embedded in the fuel matrix. This case is formulated considering a congruent dissolution of the matrix [14 and 24]. Here, the nuclides are liberated from the matrix as the matrix dissolves. As the matrix consists mainly of uranium dioxide, the rate N_c at which the embedded nuclides are liberated depends on the uranium dissolution rate N_u and on the nuclide fraction in the fuel matrix. This process is formulated as:

$$N_c = N_u \frac{M_{i, \text{matrix}}}{M_{u, \text{matrix}}} \quad (12)$$

where $M_{i, \text{matrix}}$ and $M_{u, \text{matrix}}$ are the amounts (moles) of the embedded nuclide and the uranium dioxide in the fuel matrix, respectively. The material balance for the nuclide in the fuel matrix is expressed as:

$$\frac{dM_{i, \text{matrix}}}{dt} = -N_c - M_{i, \text{matrix}} \lambda \quad (13)$$

The dissolution rate term N_c is included as a production term in the equations defining the source.

4.2 APPROACHES USED BY THE MODEL

The elements required to define the compartmentalization are the geometry and dimensions of the system, and the properties of the materials through which the nuclides migrate. The compartments are defined by their volume, their diffusion length and cross-sectional area used by the diffusion. Conceptually, the model uses a rather straightforward compartmentalization process. This coarse compartmentalization could yield poor or even meaningless numerical results. To avoid this, analytical or semi-analytical solutions are introduced into the model in the zones where a finite difference scheme would require a fine discretization. Some of the approaches used by the model to describe the solute transport are described in the following sections.

Transport into a Large Compartment

Species diffusing out of a small hole into a very large volume of material spread out spherically. Very near the hole, the cross-section is still of the order of the size of the hole. Further away, the cross-section increases considerably as the "sphere" grows. Thus, most of the resistance to diffusion is concentrated very near the mouth of the hole. For the situation depicted in KBS-3, diffusive transport from a small hole in the canister wall into the bentonite, the resistance to the diffusive transport is then replaced by a plug with an equivalent resistance as shown in Figure 8.

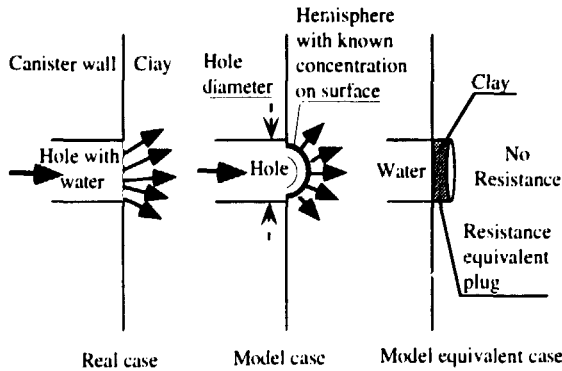


Figure 8 A schematic view of the real case and the model case that are used to obtain the resistance-equivalent plug.

This resistance is calculated by integrating the transport rate equation, $N = -2\pi r^2 D_c \frac{dc}{dr}$, from a small hemisphere into a very large volume, between the limits of the sphere of radius r_{sph} and an outer radius r . Since the species spread over a large volume in the surrounding medium $r \gg r_{sph}$, the nuclide transport rate simplifies to $N = 2\pi r_{sph} D_c \Delta c$. In the model depicted in Figure 8, the real situation is approximated by using an equivalent plug. This plug of a cross-sectional area equal to the hole area has a thickness Δx given by $\Delta x = r_{hole} \sqrt{2}$.

Transport into a Narrow Slit

For diffusive transport into a narrow fracture, most of the resistance to the transport is located nearest to the fracture because of the contraction in the cross-sectional area. The transport resistance is then approximated by a plug through which the nuclides are transported. The plug has a transport area equal to the cross-sectional area of the fracture, and a diffusion length equal to a factor times the fracture aperture. Neretnieks analytically modelled the stationary transport from the bentonite surrounding a canister for spent nuclear fuel into a

fracture [25]. The procedure uses the exact solution of the steady-state two-dimensional diffusion equation for a sector of the clay barrier representing half the fracture spacing which allows symmetry conditions to be used. After some simplifications, the resistance of the plug at the mouth of the fracture is expressed as $R_f = \left[(F_{x,0}/\delta) \delta / (D_c A_f) \right]$.

The factor $F_{x,0}/\delta$ was calculated by Neretnieks for a number of fracture spacings, fracture apertures and barrier thicknesses. For fractures with an aperture varying between 10^{-4} and 10^{-3} m, and a backfill thickness of 0.30 to 0.35 m, the factor ranges between 3 and 7. It can be visualized as having a plug of clay at the mouth of the slit with a thickness of $F_{x,0}/\delta$ times the slit aperture.

Transport into the Flowing Water

For compartments in contact with water flowing in fractures in the rock, the diffusive transport is determined by an equivalent flow rate Q_{eq} . This parameter represents a fictitious flow of water which carries with it a concentration equal to that at the compartment interface. It has been derived by solving the equations for diffusional transport to the passing water by boundary layer theory [26]. This entity is obtained from:

$$Q_{eq} = U_o \cdot W \cdot \bar{\eta} = U_o \cdot W \cdot \sqrt{\frac{4 \cdot D_w \cdot t_w}{\pi}} \quad (14)$$

where W is the width of the compartment in contact with water flowing in fractures, fracture zones or damaged zones, and $\bar{\eta}$ is the mean thickness of penetration into the water by diffusion from the compartment. The residence time, t_w , is the time that the water is in contact with the compartment. This time is obtained from the flux of water U_o , the flow porosity, and the length of the pathway in contact with water.

4.3 MANAGING THE MATERIAL BALANCE IN THE COMPARTMENTS

The terms determining the material balance for the compartment are: the rate at which the species are transported to the adjacent compartments, degradation by decay, dissolution of the solid inventory and the accumulation of the species in the compartment. To account for the solid inventory, the physical compartment is defined by two fictitious subcompartments; one to handle the solid inventory and the other to handle the species dissolved in the water and sorbed in the solid material.

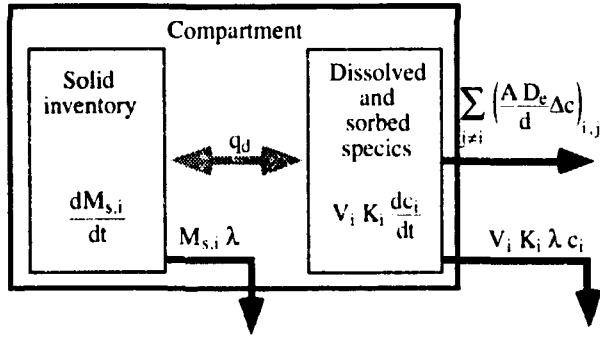


Figure 9 A schematic view of the processes occurring in a compartment for a single nuclide. The compartment is described by two fictitious subcompartments.

The two subcompartments are coupled by a dissolution term q_d , see Figure 9. A change in the solid inventory M_s with time is determined by the degradation of the inventory by decay, and the dissolution of this into the water. This is formulated as:

$$\frac{dM_{s,i}}{dt} = - M_{s,i} \lambda - q_d \quad (15)$$

and the formulation for the dissolved and sorbed species is:

$$V_i K_i \frac{dc_i}{dt} = q_d - V_i K_i c_i \lambda - \sum_j \left(\frac{A D_e}{d} \Delta c \right)_{i,j} \quad (16)$$

where the left-hand side is the change in mass in the porous material, and the terms on the right-hand side are for the dissolution of the solid, the degradation of the dissolved and sorbed species by decay, and rate at which the species are transported away by diffusion. The term Δc is defined as the concentration difference between two adjacent compartments $\Delta c_{i,j} = c_i - c_j$.

Basic Equations for Radionuclide Chains

The present model considers only the migration of radionuclide decay chains of the form $A \rightarrow B \rightarrow C \rightarrow \dots \rightarrow N$. The mathematical handling for a nuclide chain is very similar to the formulation describing the release of a single nuclide. For a nuclide chain, the material balance over a compartment is described by a set of linear differential equations. The calculations for the members in the chain are made in succession, beginning with the first member of the chain, the mother nuclide. The mother nuclide is independent of the other

nuclides in the chain. The decay term for a parent is a source term for a daughter nuclide and is included as such in the calculations for the daughter.

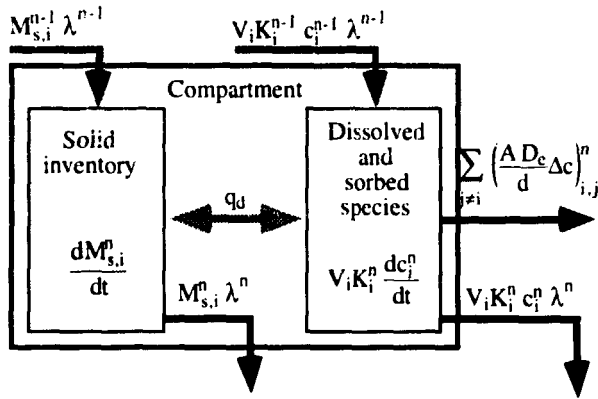


Figure 10 A schematic view of the processes occurring in a compartment for the daughter nuclide.

The solid inventory balance M_s is determined by the production of solid by decay of a parent nuclide, the degradation of the solid by decay, and the solid dissolution into the liquid phase q_d as it is schematized in Figure 10. For nuclide "n" in compartment "i", the solid balance is:

$$\frac{dM_{s,i}^n}{dt} = M_{s,i}^{n-1} \lambda^{n-1} - M_{s,i}^n \lambda^n - q_d \quad (17)$$

and for the dissolved and sorbed species it is:

$$V_i K_i^n \frac{dc_i^n}{dt} = q_d + V_i K_i^{n-1} c_i^{n-1} \lambda^{n-1} - V_i K_i^n c_i^n \lambda^n - \sum_j \left(\frac{A D_e}{d} \Delta c \right)_{i,j}^n \quad (18)$$

These equations are very similar to the governing equations for a single nuclide, except for the term for the production from the preceding nuclide in the chain. The initial conditions and constraints for the compartments are handled in the same way as for single nuclides.

4.4 VERIFICATION OF THE MODEL

Verification is addressed by comparing the results given by the model with known analytical solutions and by comparison with an independent numerical code. Here, the accuracy of the steady state and transient solutions given by the code NUCTRAN for this model has been investigated by defining test cases. Analytical solutions were used to verify the numerical solution and the steady state solution of NUCTRAN [27 and 28]. For the verification of the non-stationary solution, a well-verified numerical code TRUMP-code [29 and 30] is used. TRUMP is a computer program used to solve mass and heat transfer problems. A detailed description of the NUCTRAN-verification exercise is documented in Paper III.

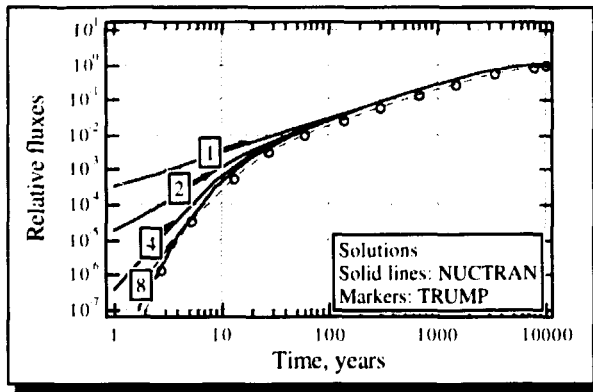


Figure 11 The relative fluxes are given for various subdivisions of the cylinder into compartments, when the access and escape of the nuclides occur through small holes. Numbers on the curves indicate the number of compartments used in the calculations.

A verification test simulating the nuclide transport escaping from the canister into the bentonite in the KBS-3 repository is shown in the following example. The solute transport for various compartmentalizations of a solid cylinder is calculated. The transport at the ends of the cylinder occurs through small circular holes through which the solute enters and leaves the solid cylinder. The cross-sectional area of the hole or plug is very small and the concentration of the solute in the hole is constant. The calculations for this test case are summarized in Figure 11.

Comparison of results showed that the accuracy of the compartment model is good compared with that of models that use a very detailed discretization. When mass transport is dominated by resistances at sensitive points, accurate results are obtained with a few compartments as shown in Figure 11. For long-lived nuclides, no large error in the release rate is expected. For the short-lived nuclides, the solution obtained may be somewhat erroneous at short times but the error may be greatly diminished by a subdivision of the large compartments at the sensitive zones. Figure 11 shows that considerable improvement in accuracy is gained if

large compartments are subdivided into two or four compartments. A finer subdivision improves the accuracy only slightly.

4.5 ILLUSTRATIVE CALCULATIONS

As an illustration of the capability of the model, the Np-229 release and a radionuclide chain release from the KBS-3 repository are calculated.

To calculate the radionuclide release the model requires: a) data on the nuclides such as diffusion, sorption, half-life, solubility and inventory, b) data on the backfill materials such as porosity and density, c) data on the sinks such as the equivalent water flow rates and d) data on the geometry and dimensions of the system. The results obtained using this model are the nuclide release through the various pathways, the concentrations in all compartments and the variation in the nuclide inventory in the source. Information on the required data can be found in Tables A1 and A2 in the Appendix. The geometrical dimensions of the repository of interest for the compartmentalization of the system are: the canister with a diameter of 0.8 m, a length of 4.5 m, a thickness wall of 0.06 m, and a hole size at the canister wall of 5 mm²; the deposition hole 7.5 m long and with a diameter of 1.5 m; the tunnel with a cross-sectional area of 3.2 x 4 m² and a distance between the centre of two canisters of 6 m.

The compartmentalization of the KBS-3 repository reduces to 13 compartments, enough to obtain an acceptable accuracy in the release of long-lived nuclides. This number may be increased if at short time a larger accuracy is needed, as shown in Figure 11. The coarse compartmentalization of the repository is discussed in Paper IV. The results of this exercise are shown in Figures 12 and 13.

The results for the Np-237 are shown in Figure 12. The neptunium in the canister diffuses through the hole into the bentonite and then migrates through the four possible pathways (Q1 to Q4 in Figure 1) into the water flowing in the rock. From the top graph we can predict that less than 2% of the neptunium escaping from the canister leaves the repository and that most of the release is preferentially through the fracture intersecting the deposition hole path-1, i.e. the shortest path. Later, the release is preferentially through path-1 and through the disturbed zone path-2. The graph illustrating the variation in concentration with time for specific zones in the repository shows a large retarding effect on the concentration in the zones far from the bentonite. The retarding effect is mainly due to the high sorption capacity of the bentonite for this nuclide. It takes over 1 million years for the concentration in the bentonite to reach the maximum value.

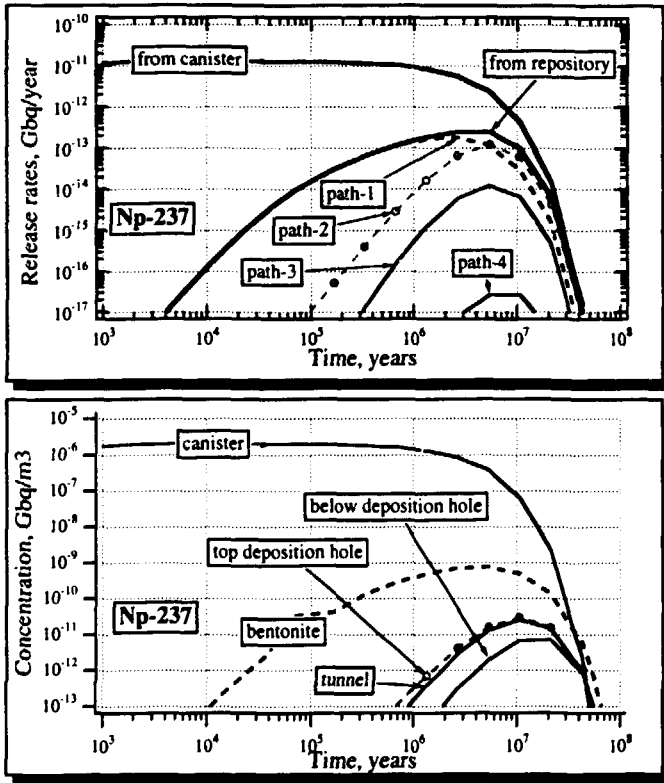


Figure 12 Calculations in the KBS-3 repository for Np-237 using the congruent approach for the dissolution of the matrix.

The results for the chain $U-238 \Rightarrow U-234 \Rightarrow Th-230 \Rightarrow Ra-226$ are shown in Figure 13. The Ra-226 shows the highest release from the repository, even higher than that of the uranium that is the generate-source of radium. A fraction of the Ra-226 is transported through the barrier system as U-238. Once again, the role of the sorption in the materials for the release is shown. The radium has a much lower sorption coefficient than the uranium and therefore a higher activity in the pore water of the compartments is obtained. If the transport properties in all materials were the same, a secular equilibrium would be obtained. It means that the activity release rates of the parent nuclide U-238 and the daughters are equal.

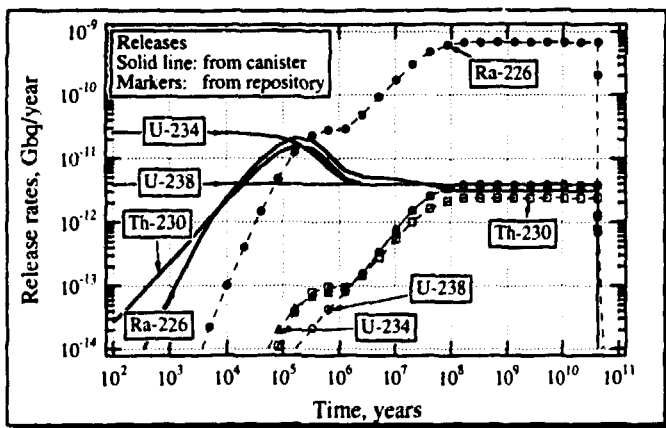


Figure 13 Calculations in the KBS-3 repository for a nuclide chain.

4.6 DISCUSSION OF THE MODEL

The model may handle the inventory of the species in the canister in two ways, using a solubility limit approach or a congruent dissolution approach. The solubility limit approach is used for nuclides free from the fuel matrix. If the approach is used for nuclides embedded in the matrix, it overestimates the release rate from the repository. Thus, for nuclides embedded in the matrix, the approach may be considered to be quite conservative. On the other hand, the congruent approach for nuclides embedded in the matrix gives more realistic results, but this approach is based on a simplification of the dissolution of the matrix that could be a much more complex process (see Section 2.2).

The compartmentalization of the geometrical system is very coarse and rather simple. For the specific case of the KBS-3 repository, the use of this coarse compartmentalization (<20 compartments) does not largely influence the accuracy of the results. The coarse compartmentalization is made possible by embedding analytical solutions at critical points. In the KBS-3 repository, these locations control the release and therefore the accuracy of the release is not greatly affected by the coarse compartmentalization.

The model has shown its capability by calculating the non-stationary release in the KBS-3 repository and in an alternative repository of the very long tunnel type for diverse situations [31 and 32]. Applicabilities of the model are shown in Paper IV. The accuracy of the model when applied to the KBS-3 is quite good and is sufficient in many cases using of the order of 20 to 30 compartments, considering that uncertainties in the location of fractures, the size of the damage, etc. may be considerably larger. A sensitivity analysis has been made in order to quantify uncertainties regarding the release. This is described in the following section.

5 IMPACT OF THE UNCERTAINTIES IN THE PARAMETERS ON THE RELEASE

In the Swedish KBS-3 repository, radionuclide transport occurs mainly by diffusion through four main barriers. The first barrier is the fuel matrix itself, which consists of pellets of 95% of uranium dioxide crystals. Incorporated in the crystals are other radionuclides such as fission products and actinides that are liberated as the crystals dissolve. This process is controlled by the rate at which the uranium can be transported away from the canister and by the uranium solubility that limits the uranium escape rate. The second barrier is the copper canister from which the radionuclides diffuse into the bentonite. The third barrier is the backfill material, where the transport of some nuclides may be strongly retarded by sorption. The fourth barrier is the fractured rock surrounding the repository, where the nuclide may be retarded.

In many of the properties or parameters defining these barriers, there is a natural variability and often an uncertainty in, e.g., the size of the damage at the canister wall, flow rates in the channels, locations of fractures intersecting the repository, diffusion and sorption coefficients, etc. These uncertainties may give an inaccurate release to the far field.

5.1 ENTITIES INFLUENCING RADIONUCLIDE TRANSPORT IN THE NEAR FIELD

The nuclide transport depends mainly on the chemical and diffusive properties of the nuclides, and sorption on the various materials by which the nuclides migrate. Other entities that strongly influence the release to the far field are the geometry and the water flow rates in channels intersecting the repository. A short description of the main parameters or variables affecting the release is given as follows:

The damage in the canister wall is assumed to be a very small hole, so there will be a large resistance controlling the nuclide escape rate from the canister. As the copper canister is resistant to corrosion, no large growth of the hole is expected for the copper/lead canister studied here [5]. In many situations, the hole size controls the nuclide transport in the repository. If for some reason the canister loses its integrity, the nuclide transport is no longer controlled by the small hole. The control of the nuclide transport is then shifted to the backfill or to the water flow rate in the fractures in the rock.

The solubility of the nuclides limits the concentration in the canister and the rate of release of the species escaping from the canister. Solubility is used in the performance assessment of the near field to establish the upper limit of radionuclide release from the waste matrix through the canister (source term). The solubility of the nuclides may be altered by possible changes in the redox potential in the repository. Under oxidizing conditions, uranium dioxide and other redox-sensitive elements are oxidized to a higher oxidation state and become more soluble.

The diffusion coefficient, D_e , controls the migration of the radionuclides through the various barriers to the flowing water in the rock. Diffusion in near-field materials is an entity that has been much studied and is expected to have a low uncertainty.

The sorption coefficient k_d determines the capacity of the material to delay the mobility of the nuclides. If the transport of a short-lived nuclide is delayed by sorption, the nuclide may

decay to insignificant concentrations before it reaches the flowing water in the fractures in the rock. The sorption for some nuclides is sensitive to changes in the redox potential of the medium. If this potential stays unchanged, a low uncertainty in the sorption coefficient is expected.

The hydraulic properties of the rock, such as water flux, channel frequency and flow distribution, aperture of the channels, etc., define the nuclide transport between the backfill and the mobile water in the fractures in the rock. The channel aperture determines the contact area between the mobile water and the backfill through which the nuclides access the mobile water. The channel frequency may have a great impact on the near field release to the far field. If a few channels only are present in the rock, many canisters may in practice have no access to mobile water. The water flow rate distribution is also important, because some canisters may be intersected by channels with high water flow rates. Measurements of channel frequency and water flow rate may present considerable difficulties and their values may vary considerably. This hydraulic information about the rock is used to determine the equivalent flow rate, Q_{eq} an entity that is used to account for the diffusive transport into the flowing water in the fractures in the rock.

5.2 PARAMETER SENSITIVITY ANALYSIS

In order to quantify uncertainties regarding the release to the far field, a sensitivity analysis has been performed with respect to the uncertainties in the parameters governing the release. The methodology used is easy to grasp and quickly conveys the important issues. It assumes that uncertainties in the release from parameter interaction are negligible. First, the overall performance model, which assesses the maximum nuclide release rate from the repository in terms of the best estimates of parameters is established. This overall performance model is defined as the central case. Second, by varying each parameter individually by a factor according to its variability, the relative change in release rate related to the central case is calculated for each of the parameters. This relative change shows the effect of the uncertainty in the parameter on the nuclide release. Finally, the logarithms of the relative maxima are plotted versus their corresponding variability factors.

For the analysis, a few nuclides have been chosen, considering the half-life and the capacity of sorption and diffusion in the backfill material. They are the fission products strontium, cesium and iodine and the actinides plutonium and uranium. The group of nuclides belonging to the fission products has a high solubility whereas the other group presents solubility limitations.

Data Used to Determine the Central Release-values

For the safety analysis of the KBS-3 repository, best estimated values and conservative values based on experimental data have been proposed for most nuclides of interest. Table A1 in the Appendix shows values for diffusivity, sorption, and solubility data in saline water and reducing conditions. These values, significant with respect to safety of the final disposal, lead with a high probability to an overestimation of radiation doses in the biosphere. Data on equivalent flow rates are found in Table A2. The uncertainties between parameters may differ widely, e.g., the flow rates in the disturbed zone and in the channels intersecting the deposition hole may vary by two or more orders of magnitude, whereas the diffusivity and sorption in the bentonite surrounding the canister is expected to have an uncertainty of not more than a factor of two or three. Data on factors of variability of the parameters based on expected variations are also found in Tables A1 and A2.

The releases of the soluble fission nuclides cesium strontium and iodine are calculated. The calculations for these nuclides consider only the fraction in the fuel/cladding gap that is rapidly transported from the canister, 10% of the total inventory. The other fraction, not considered, is embedded in the matrix and therefore its release is slow in comparison to the fraction in the fuel/cladding gap. In the case of the plutonium, the calculations take into account the fact that this nuclide is embedded in the uranium dioxide matrix.

Summary of the Results

The results of the sensitivity analysis are summarized in two figures: Figure 14 showing the effect of uncertainties in the parameters on the peak radionuclide release to the far field and Figure 15 showing the radionuclide release distribution for the central case for some representative nuclides.

The effect of uncertainties in the parameters on the release cannot be generalized for all nuclides, but some patterns of their influence can be given. Variations in the size of the damage in the canister wall have a strong influence on the release. Variations in uranium solubility have a strong influence on the release of those nuclides that are embedded in the uranium dioxide matrix. Variations in the nuclide's own solubility is only important for those nuclides that may be considered to be free from the matrix. Variations in the adsorption capacity of the bentonite surrounding the canister and in the equivalent flow rate in the fractures in the rock nearest to the canister, e.g. a fracture intersecting the deposition hole and disturbed zone, have a strong influence on the release. Therefore, parameters such as hole size, uranium solubility, sorption, and equivalent flow rates have to be accurately determined in order to minimize uncertainties in the release to the far field. For nuclides with a high diffusion coefficient in the bentonite, e.g., cesium and strontium, the hydraulic properties of the fractured rock nearest to the deposition hole have to be well determined. For the iodine, on the other hand, with a very low diffusion coefficient, uncertainties in the hydraulic properties of the near-field rock have a very small effect on the release. For the iodine, uncertainties in the release arise from variations in diffusivity. The uranium release, with a very high inventory, is not affected by uncertainties in

the hydraulic properties of the rock.

The released nuclide fraction through each pathway is not greatly influenced by uncertainties in the transport properties of the backfill materials, whereas uncertainties in the water flow rates in the fractures have a strong influence on the peak nuclide release distribution.

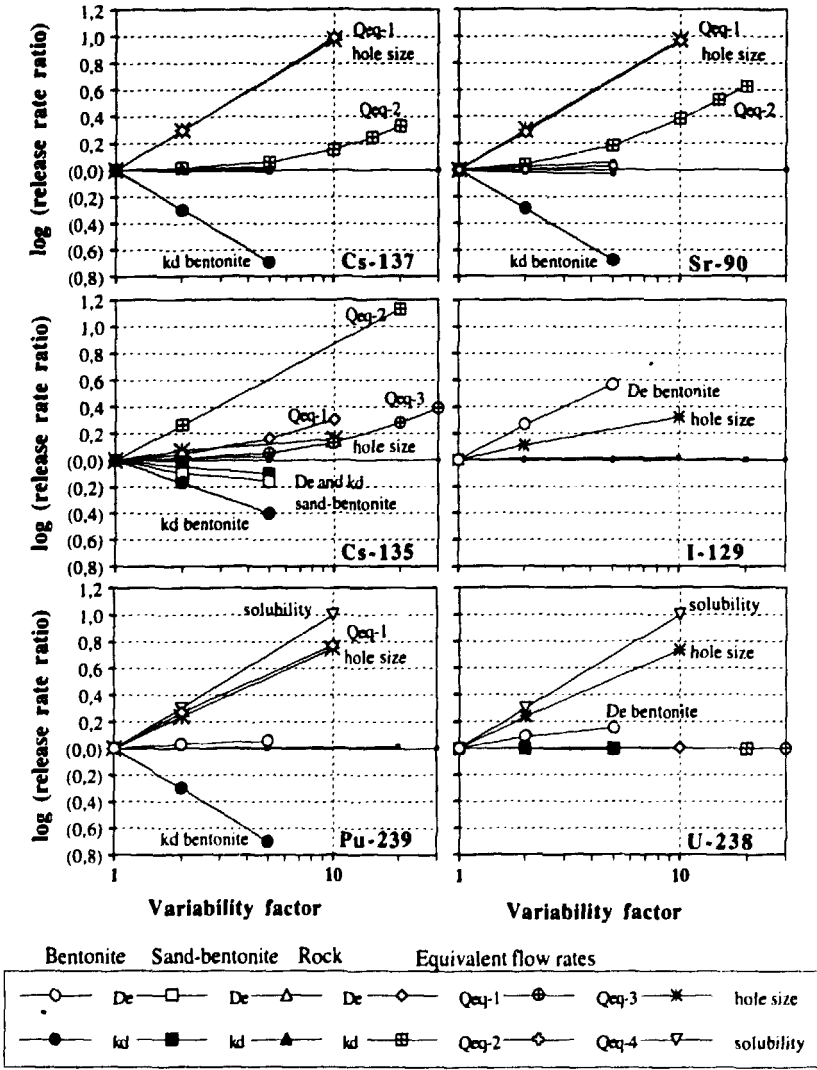


Figure 14 Impact of the uncertainties in the parameters on the peak radionuclide release from the KBS-repository.

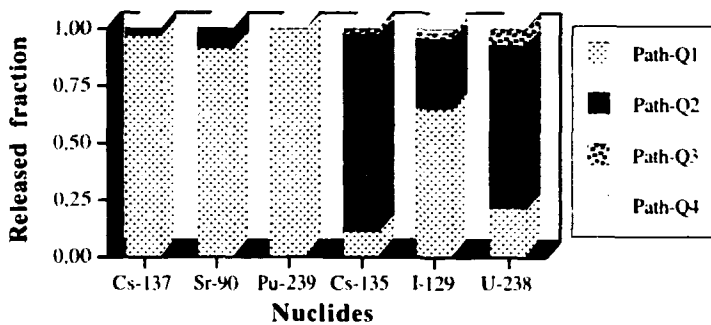


Figure 15 The radionuclide release distribution is given for the central case that is defined by the central parameter-values. The released fractions are determined when the release rate reaches its maximum value.

5.3 DISCUSSION OF THE UNCERTAINTIES IN THE RELEASE

Uncertainties in the calculated release of nuclides escaping from the repository arise from uncertainties in the parameter-values governing the nuclide transport in the repository and from uncertainties due to the model itself.

The sensitivity analysis showed that uncertainties in some parameter-values have a strong influence on the release. A factor 10 of uncertainty in release may be found. This factor is comparable to the uncertainties in the parameter-values that range between 5 for the transport properties and 30 for the hydraulic properties of the rock.

Uncertainties arising from the model itself may have different sources. One source may be the description of the scenario concerning the location of the hole in the canister wall, the location of the fracture intersecting the deposition hole, the number and characteristics of the pathways by which the nuclides are transported, etc. Another source may be assumptions relating to the mechanisms involved in the rate of dissolution of the waste matrix and in the nuclide transport through the different barriers. Model simplifications may also cause uncertainty, e.g. nuclide transport in the interior of the canister, which is considered to be a well-mixed tank reactor. Another simplification is the assumption that all the capacity of the bentonite surrounding the canister is equilibrated. In fact, in the case of a small damage in the canister wall, the transport through the bentonite only occurs through a portion of it. Finally, other source of uncertainty is inherent in the numerical model, a rough discretization of the barrier system may be used by embedding analytical solutions in sensitive zones. Sources of uncertainties such as the description of the scenario, mechanisms and simplifications are handled by making conservative assumptions. Uncertainties arising from the rough discretization could be large for nuclides of short half-life. These uncertainties may, however, be greatly reduced by a subdivision of sensitive compartments.

6 CONCLUSIONS

The near field of a repository for high-level nuclear waste has been studied. The work is focused on the modelling of the redox front which originates when the oxidants in the canister escape to the surroundings and on the development of a fast and flexible model to calculate the transport of radionuclides escaping from the canister. In both cases, the KBS-3 canister is considered.

The advance of the redox front was determined for three rates of production of oxidants. The range of the predicted travelled distances of the front is from less than a metre to over a thousand metres. The long distances were, however, found for the unrealistic high radiolysis rate. The calculations were made assuming the transport of oxidants in individual channels over long distances which could also be unrealistic. It is, for example, unlikely that the redox front will ever move past the bentonite and if it does the front may move less than 100 m in a channel with a high water flow rate.

Application of the redox front model at the Poços de Caldas Natural analogue served to explain the main mechanisms and processes contributing to the formation and movement of the redox front, such as transport of the oxidants through fractures with diffusion into the rock matrix. In addition, evidence of dissolution and precipitation of redox-sensitive nuclides moving past the redox front and matrix diffusion were also found in Poços de Caldas.

The model developed to calculate the migration of radionuclides from the canister is fast and flexible. The model uses a coarse compartmentalization of the system by embedding analytical solutions in zones where other models, such as finite differences, would need a very fine discretization. The concentration of the radionuclides within the canister may be determined by the nuclide own's solubility or by congruent dissolution of the fuel matrix. A small number of compartments suffices to obtain a good accuracy in the release. For short-lived nuclides inaccurate results could be obtained, but this uncertainty is largely reduced by an increase in the number of compartments. Uncertainties in the release arising from the model are small in comparison to those arising from the variability in the parameter-values and material properties.

The sensitivity analysis showed that the variability in the parameter-values does not have the same impact on the release of all nuclides. Parameters such as hole size in the canister wall, uranium solubility, sorption, and the hydraulic properties of the fractured rock nearest to the canister have to be well known in order to minimize uncertainties in the calculated release. Variability in the material properties has no large influence on the release distribution from the repository, but the water flow rates strongly influence which path will dominate the escape route. Short-lived nuclides preferentially migrate through the shortest path and long-lived nuclides preferentially migrate to the disturbed zone around the tunnel and to a smaller extent to the fracture intersecting the deposition hole.

NOTATION

A	= cross-sectional area for diffusion (m^2)
c	= concentration (mol/m^3)
c^f	= concentration in the fracture (mol/m^3)
c^p	= concentration in the pore water in the rock matrix (mol/m^3)
D_e	= effective diffusivity (m^2/yr)
d	= diffusion length (m)
i	= stoichiometric factor for the oxidation reaction
K_i	= distribution coefficient
k_d	= sorption coefficient (m^3/kg)
M	= solid inventory (mol)
N	= dissolution rate or production rate (mol/yr)
Q_{eq}	= equivalent water-flow rate (m^3/yr)
q	= concentration of the oxidized reducing species in the solid (mol/m^3)
q_0	= initial concentration of the reducing species in the solid (mol/m^3)
r	= radius (m)
S	= thickness of the slab or spacing between fractures (m)
T_1	= breaching time of the canister (yr)
T_2	= time at which the redox front reaches the fracture (yr)
t	= time (yr)
U_0	= flux of water ($m^3/m^2 \cdot yr$)
u	= water velocity (m/yr)
u_0	= infiltration flux (Darcy velocity) ($m^3/m^2 \cdot yr$)
V	= volume (m^3)
v_f	= velocity of the redox front (flow direction) (m/yr)
W	= width (m)
x	= distance (diffusion direction) (m)
x_f	= location of the redox front (m)
z	= distance (flow direction) (m)

Greek

δ	= fracture aperture (m)
ϵ_p	= porosity
η	= mean penetration thickness (m)
λ	= decay constant (yr^{-1})
ρ	= density (kg/m^3)

REFERENCES

- 1 W. Miller, R. Alexander, N. Chapman, I. McKinley, and J. Smellie, "Natural Analogue Studies in the Geological Disposal of Radioactive Wastes," *Studies in Environmental Science* 57, Elsevier, Amsterdam, (1994).
- 2 "Final storage of spent nuclear fuel," KBS-3, Swedish Nuclear Fuel Supply Company, (1983).
- 3 P. Wikberg, I. Grenthe, and K. Axelsen, "Redox Conditions in Groundwaters From Svartboberget, Gideå, Fjällveden and Kamlunge. Kärnbränsle-Säkerhet," TR 83-40, Swedish Nuclear Fuel and Waste Management Company (1983).
- 4 B. Torstenfelt, B. Allard, W. Johanson, and T. Ittner, "Iron Content and Reducing Capacity of Granites and Bentonite," TR 83-36, Swedish Nuclear Fuel and Waste Management Company (1983).
- 5 "Final Disposal of Spent Nuclear Fuel. Importance of the Bedrock for Safety," SKB-91, TR 92-20, Swedish Nuclear Fuel and Waste Management Company (1992).
- 6 L. Werme, P. Sellin, and N. Kjellbert, "Copper Canister for Nuclear High Level Waste Disposal. Corrosion Aspect," TR 92-26, Swedish Nuclear Fuel and Waste Management Company (1992).
- 7 O. Karnland and R. Push, "Development of Clay Characterization Methods for Use in Repository Design with Application to a Natural Ca Bentonite Clay Containing a Redox Front," TR 90-42, Swedish Nuclear Fuel and Waste Management Company (1990).
- 8 K. Palmqvist and R. Stanfors, "The Kymmen Power Station TBM Tunnel. Hydrogeological Mapping and Analys," TR 87-26, Swedish Nuclear Fuel and Waste Management Company (1987).
- 9 H. Abelin, L. Birgersson, J. Gidlund, L. Moreno, I. Neretnieks, H. Widén, and T. Ågren, "3-D Migration Experiment-Report 3, Part I, Performed Experiments, Results And Evaluation," Stripa project Technical Report 87-21, Stockholm, Nov. (1987).
- 10 I. Neretnieks, H. Abelin and L. Birgersson, "Some Recent Observations of Channeling in Fractured Rocks. Its Potential Impact on Radionuclide Migration," U.S. Dep. Energy - At. Energy Can. Ltd. Conf., San Francisco, CA, Proc., p.315-335, Sept 15-17 (1987).
- 11 L. Moreno, Y.W. Tsang, C.F. Tsang, F.V. Hale, and I. Neretnieks, "Flow and Tracer Transport in a Single Fracture. A Stochastic Model and its Relation to Some Field Observations," *Water Resources Research* 24, p. 2033-3048, (1988).

- 12 H. Abelin, L. Birgersson, H. Widén, T. Ågren, L. Moreno, and I. Neretnieks, "Channeling Experiment to Study Flow and Transport in Natural Fractures," *Journal of Contaminant Hydrology*, 15, p. 129-158, (1994).
- 13 L.H. Johnson, D.W. Shoesmith, and S. Stroes-Gascoyne, "Spent Fuel: Characterization Studied and Dissolution Behaviour under Disposal Conditions," *Mat. Res. Soc. Symp. Proc.* 112, 99 (1988).
- 14 F. Garisto and N.C. Garisto, "Source Term Models for the Release of Radionuclides from used Nuclear Fuel," In TR 91-59, Swedish Nuclear Fuel and Waste Management Company (1991).
- 15 J. Bruno and P. Sellin, "Radionuclide Solubilities To Be Used in SKB 91," TR 92-13, Swedish Nuclear Fuel and Waste Management Company (1992).
- 16 H. Christensen and E. Bjergbakke, "Radiolysis of Groundwater from Spent Fuel," TR 82-18, Swedish Nuclear Fuel and Waste Management Company (1982).
- 17 I. Neretnieks and M. Faghihi, "Some Mechanisms Which May Reduce Radiolysis," TR 91-46, Swedish Nuclear Fuel and Waste Management Company (1991).
- 18 I. Neretnieks, "The Movement of a Redox Front Downstream from a Repository For Nuclear Waste," *Nuclear Technology*, 62, p. 110, (1983).
- 19 D.C. Holmes, A.B. Pitty and D.J. Noy, "Geomorphological and Hydrogeological Features of the Poços de Caldas Caldera, and the Osamu Utsumi Mine and Morro do Ferro Analogue Study Sites, Brazil," In Poços de Caldas Technical Report No. 5, NAGRA/ SKB/ UKDOE, 1991.
- 20 N. Chapman, I. McKinley, M. Shea, and J. Smellie, "The Poços de Caldas Project: Summary and Implications for Radioactive Waste Management," In Poços de Caldas report No. 15, NAGRA/ SKB/ UKDOE, 1991.
- 21 J. Liu and I. Neretnieks, "Some Evidence of Radiolysis in an Uranium Ore Body - Quantification and Interpretation," MRS-94 Scientific Basis for Nuclear Waste Management XVIII, Kyoto, Japan, Oct. 25-29 (1994).
- 22 T.N. Narasimhan and P.A. Witherspoon, "An Integrated Finite Difference Method for Analyzing Fluid Flow in Porous Media," *Water Resour. Res.*, 12, p. 57-64, (1976).
- 23 D. Kahaner, C. Moler, S. Nash, "Numerical Methods and Software," Prentice Hall, (1988).

- 24 I. Neretnieks, "Diffusivities of Some Constituents in Compacted Wet Bentonite Clay and the Impact on Radionuclide Migration in the Buffer," *Nuclear Technology*, 71-458, (1985).
- 25 I. Neretnieks, "Stationary Transport of Dissolved Species in the Backfill Surrounding a Waste Canister in Fissured Rock: Some Simple Analytical Solutions," *Nuclear Technology*, 72-194, (1986).
- 26 I. Neretnieks, "Transport Mechanism and Rates of Transport of Radionuclides in the Geosphere as Related to the Swedish KBS-Concept," *Proc. Symp. Underground Disposal of Radioactive Wastes*, Otaniemi, Finland, July 2-6, 1979, Vol II. p 108, International Atomic Energy Agency (1979).
- 27 J. Crank, "The Mathematics of Diffusion," 2nd ed. Oxford University Press New York, (1975).
- 28 H.S. Carslaw and J.C. Jaeger, "Conduction of Heat in Solids," 2nd ed. Oxford University Press, New York, (1959).
- 29 A.L. Edwards, "TRUMP: A Computer Program for Transient and Steady State Temperature Distributions in Multidimensional Systems," Report, Natl. Tech. Inf. Serv., Nat. Bur. of Standards, Springfield (1969).
- 30 A. Rasmuson, T.N. Narasimhan, and I. Neretnieks, "Chemical Transport in a Fissured Rock: Verification of a Numerical Model," *Water Resour. Res.*, Vol 18, 5, p. 1479-1492, (1982).
- 31 L. Romero, L. Moreno, and I. Neretnieks "Release Calculations in a Repository of the Very Long Tunnel Type," TR 92-29, Swedish Nuclear Fuel and Waste Management Company (1992).
- 32 L. Romero, I. Neretnieks, and L. Moreno, "Release of Radionuclides from the Near Field by Various Pathways. The Influence by the Sorption Properties of Materials in the Near Field," In *proceedings Scientific Basis for Nuclear Waste Management XV*, Strasbourg, Nov 4-7, 1991, Ed. C. G. Sombret, pp 699-704 (1992).
- 33 F. Brandberg and K. Skagius, "Porosity, Sorption and Diffusivity Data Compiled for the SKB 91 Study," TR 91-16, Swedish Nuclear Fuel and Waste Management Company (1991).
- 34 M. Wiborgh and M. Lindgren, "Database for the Radionuclide Transport Calculations for SFR," Progress report SFR 87-09, Swedish Nuclear Fuel and Waste Management Company (1987).

APPENDIX: Tables

Table A1 Best Estimates of Parameters in a Saline and Reducing Environment as Used in SKB-91 [2, 5, 8, 20].

Nuclide	Inventory	Solubility	Half-life	Bentonite		Sand-Bentonite		Rock	
				D_e	k_d	D_e	k_d	D_e	k_d
I-129	2.22	high	1.57×10^7	2.5×10^{-12}	0	10^{-10}	0	10^{-13}	0
Cs-135	4.55	high	2.95×10^6	2.5×10^{-8}	0.05	2.8×10^{-9}	0.025	10^{-13}	0.05
Cs-137	6.18	high	30.1	2.5×10^{-8}	0.05	2.8×10^{-9}	0.025	10^{-13}	0.05
Sr-90	4.04	high	28.8	2.5×10^{-8}	0.01	2.4×10^{-9}	0.032	10^{-13}	0.05
Pu-239	28.05	2×10^{-8}	24 100	10^{-10}	3	10^{-10}	0.1	10^{-13}	3
U-238	5 603	2×10^{-7}	4.47×10^9	10^{-10}	3	10^{-10}	0.1	10^{-13}	3
U-234	2.03	2×10^{-7}	2.45×10^5	10^{-10}	3	10^{-10}	0.1	10^{-13}	3
Th-230	10^{-4}	2×10^{-10}	8×10^4	10^{-10}	3	10^{-10}	0.32	10^{-13}	3
Ra-226	2×10^{-8}	2×10^{-7}	1.6×10^3	2.5×10^{-8}	0.01	2.4×10^{-9}	0.032	10^{-13}	0.05
Np-237	3.03	2×10^{-8}	2.14×10^6	10^{-10}	3	10^{-10}	0.01	10^{-13}	0.01
Variability factor		10		5	5	5	5	5	5

Note: initial nuclide inventory per canister in (mol), solubility c_s in (mol/l), half-life (yr), effective diffusion coefficient D_e in (m^2/s), sorption coefficient k_d in (m^3/kg).

Table A2 Equivalent Flow Rates Q_{eq} in the Various Sinks [9] (Q1 to Q4 see Fig. 1) and Material Properties.

	Fracture in		Disturbed	Fracture
	Deposition hole	Tunnel	Zone	Zone
	Q1	Q2	Q3	Q4
Equiv. flow rate (l/yr)	0.25	0.5	4	6
Variability factor	10	30	20	30
	Material			
Material Property	Bentonite	Sand-Bentonite	Rock	
Solid Density (kg/m^3)	2 700	2 280	2 700	
Porosity (%)	25	24	0.5	